Electrochimica Acta 396 (2021) 139222

Contents lists available at ScienceDirect

Electrochimica Acta

journal homepage: www.elsevier.com/locate/electacta

Cu(111) single crystal electrodes: Modifying interfacial properties to tailor electrocatalysis

Andrea Auer[a], Francisco J. Sarabia[b], Christoph Griesser[a], Víctor Climent[b,*], Juan M. Feliu[b], Julia Kunze-Liebhäuser[a,*]

[a] Institute of Physical Chemistry, University Innsbruck, Innrain 52c, Innsbruck 6020, Austria
[b] Instituto Universitario de Electroquímica, Universidad de Alicante, Carretera San Vicente del Raspeig s/n,San Vicente del Raspeig, Alicante E-03690, Spain

ARTICLE INFO

Article history:
Received 24 June 2021
Revised 5 August 2021
Accepted 5 September 2021
Available online 9 September 2021

Keywords:
Cu single crystals
Adatom modification
Irreversible adsorption
In situ electrochemical scanning tunneling microscopy
Potential of maximum entropy
Laser induced temperature jump
Electrocatalysis

ABSTRACT

Tailoring electrocatalyst materials to the specific requirements of a certain reaction and to optimize activity or enhance selectivity is a key tactic for the development of low-temperature fuel and electrolyzer cells for clean energy production. Here, we demonstrate the modification of Cu(111) electrodes with different sub-monolayer coverages of foreign metals (Cd) and metal hydroxides ($Co(OH)_2$ and $Ni(OH)_2$) for application in the hydrogen evolution reaction (HER) in alkaline media. In situ electrochemical scanning tunneling microscopy (EC-STM) reveals that these modifications have a significant influence on the morphology and structure of the Cu(111) surface with its characteristics depending on both the nature and the amount of the adsorbed metal(hydroxide). $Ni(OH)_2$ and $Co(OH)_2$ on Cu(111) lead to a significant enhancement of the electrocatalytic activity towards the HER in alkaline electrolyte, whereas a decrease in activity is found for Cd modified Cu(111). These trends can be rationalized by considering the strength of the interfacial electric field and its influence on the specific interactions of the electrode with the water ad-layer close to the surface, as determined by laser-induced temperature jump measurements. This comparative study therefore provides valuable information on the structure-activity relation as well as insights on the interfacial characteristics of different bimetallic Cu electrocatalysts.

1. Introduction

The rational design of active and selective electrocatalysts has been a central theme study in electrochemistry in the past decades. One promising and feasible concept to optimize an electrode's activity is the precise modification of the topmost layers of the catalyst surface, i.e., the sites where the reaction takes place, with monolayers or sub-monolayers of foreign metals [1]. In principle, there are two main strategies to engineer the electrode surface properties with adlayers of other metals: (i) the so-called underpotential deposition (UPD) [2,3] and (ii) irreversible adsorption [4,5,6]. UPD refers to the electrochemical deposition of a metal on a different metallic substrate, which takes place from a solution of its cation at potentials that can be significantly less negative than those needed for bulk deposition [3,4]. Since this is a reversible process, it consequently implies that the adatom coverage is very much dependent on the applied potential, and achieving a constant coverage over the whole potential range of interest is difficult [4]. Irreversible adsorption, on the other hand, occurs when, by putting a solution of a certain metallic salt in contact with an electrode at open circuit potentials, a stable adatom layer forms and remains adsorbed on the substrate in a wide potential range after transfer to a solution without the corresponding ion [4,5]. In this case, the adatom coverage can be varied depending on the solution concentration or the immersion time, independently of the applied potential.

Pt-based materials decorated with (sub-)monolayer amounts of foreign metals have been extensively studied (see for example refs [1,4,6,7]). Particularly interesting systems are 3d transition metal (TM=Ni, Co, Fe, Mn) hydroxide ($TM(OH)_2$) catalysts, due to their improved activity towards the HER in alkaline electrolytes [8–10]. For $TM(OH)_2$ modified Pt(111), water dissociation is promoted through the introduced oxophilic species due to a decrease of its energy barrier [10,11]. Interestingly, the reactivity trend for the alkaline HER (Ni > Co > Mn > Fe) clearly correlates with the corresponding oxophilicity [11]. The important role of the electric field at the solid/liquid interface and the corresponding interfacial water reorganization, in particular as an activity descriptor for the

* Corresponding authors.
E-mail addresses: victor.climent@ua.es (V. Climent), julia.kunze@uibk.ac.at (J. Kunze-Liebhäuser).

https://doi.org/10.1016/j.electacta.2021.139222

HER in alkaline media, was demonstrated for Pt(111) with different amounts of $Ni(OH)_2$ [12,13]. For this system, the so-called laser-induced temperature jump method revealed a significant decrease in the electric field strength and thus a lowering of the energy barrier associated with the reorganization of the interfacial water network with increasing amounts of $Ni(OH)_2$ on the surface [12,13].

In general, this technique allows to selectively study the interfacial water adlayer and relies on nanosecond laser pulses, which induce a sudden increase in temperature at the interface [14,15]. The electrode potential response during the temperature change gives a measure of the thermal coefficient of the interfacial potential drop ($\frac{\partial \Delta \phi}{\partial T}$) at the electrified solid/liquid interface [5]. Since this coefficient is directly related to the entropy of double layer formation, the potential at which it becomes zero corresponds to the potential of maximum entropy (pme), which, in turn, is closely related to the potential of zero free charge (pzfc) [5].

In contrast to the precisely tailored Pt-based electrodes, examples of well-defined Cu model electrodes tailored with (sub-)monolayers of foreign metals are rather scarce and consist mostly of UPD studies [16,17]. This is also due to the fact that Cu is widely used as a surface modifier[3,6] rather than a substrate. Here, we therefore demonstrate the possibility of modifying Cu(111) electrodes with sub-monolayer amounts of different foreign metal hydroxides ($Ni(OH)_2$, $Co(OH)_2$) and metals (Cd), by using irreversible adsorption. In situ electrochemical scanning tunneling microscopy (EC-STM) reveals significant differences in the structure and morphology of the bimetallic Cu materials that can be rationalized by different deposition and growth mechanisms. We show that the adsorption of $TM(OH)_2$ leads to a significant enhancement of the HER activities in alkaline media. We find an unexpected trend (Co > Ni), which can be correlated with a greater decrease of the electric field strength for $Co(OH)_2$ at potentials at which the HER takes place, as determined by laser induced temperature jump measurements. For Cd modified Cu(111) on the other hand, we see a decrease in HER activity even though there is a slight shift of the pme towards more negative values, which is rationalized through a significantly more negative thermal coefficient, i.e., a higher electric field at the interface. Our study sheds light on the interfacial properties of bimetallic Cu electrocatalysts and provides evidence, that the rate of the alkaline HER is strongly affected by the facilitation of the interfacial water reorganization during charge transfer.

2. Experimental

For a full detailed description of all experimental methods please refer to the Supplementary Materials. Shortly, Cu(111) single crystal electrodes purchased from Mateck (Jülich) were mechanically polished with diamond paste (ESCIL) down to 0.25 µm and subsequently electropolished at 1.8 V vs Cu in 60% H_3PO_4. All electrochemical measurements were performed in a standard three-electrode cell configuration with a Teflon beaker fitted inside to avoid solution contact with any glassware. Either a PTFE bound activated carbon [18] or a Pd/H_2 reference electrode and a carbon rod counter electrode were used. Argon (5.0, Messer) was used to deoxygenate the 0.1 M NaOH (sodium hydroxide monohydrate, Merck, Suprapur). A commercial Keysight 5500 scanning probe microscope, placed inside a glove box (MBraun, MB 200 MOD), was used for the EC-STM measurements. An electrochemically etched and Apiezon coated tungsten wire was employed as STM tip. Quasi in situ X-ray photoelectron spectroscopy (XPS) was measured on a MulitLab 2000 instrument (ThermoFisher Scientific) equipped with a hemispherical sector analyser (Alpha 110, ThermoFischer Scientific) and a monochromatic Al K_α X-ray source. For the laser-induced temperature jump experiments a Nd-YAG laser (Brilliant B, Quantel, 532 nm) was used, as described in Refs. [5,15,19]. Approximately, a hundred transients were averaged using a Tektronix model TDS 3054B oscilloscope.

3. Results and Discussion

Figure 1 depicts cyclic voltammograms (CVs) of $Ni(OH)_2$ and $Co(OH)_2$ modified Cu(111) with two different coverages, i.e., 0.1 and 0.2 monolayers (ML), in 0.1 M NaOH. All potentials are given versus the reversible hydrogen electrode (RHE). The voltammogram of bare Cu(111) is shown as a reference (black lines). For both voltammetric responses of Cu(111) modified with $Ni(OH)_2$ and $Co(OH)_2$ (Figure 1a and b), a decrease can be observed with increasing coverages in the distinct peak pair, associated with hydroxide (OH) adsorption and desorption on the Cu(111) surface at around 0.12 V_{RHE} [20,21]. As stated in our previous work [22], the well-defined, reversible OH adsorption feature in the CV allows to estimate the degree of blockage of the Cu surface and consequently the apparent coverage from the remaining charge density (see Figure S1 and Table S1 in the Supporting Information (SI)). This consistently yields apparent coverages of around 0.1 ML and 0.2 ML for both $Ni(OH)_2$ and $Co(OH)_2$ by the use of 10^{-4} and 10^{-2} M Ni^{2+} and Co^{2+} solutions, respectively. Although there exist uncertainties in the used coverage determination due to the unknown ratio of adsorbed adatom and OH species, clearly the charge of the fingerprint OH adsorption feature relatively decreases with increasing $Ni(OH)_2$ and $Co(OH)_2$ surface concentrations.

To determine the influence of $Ni(OH)_2$ and $Co(OH)_2$ on the electrocatalytic properties, the HER activities in alkaline media were investigated and are depicted in Fig. 1c and d. A clear enhancement can be observed for both 0.2 ML $Ni(OH)_2$ and $Co(OH)_2$ on Cu(111), whereas only a small activity increase is found for 0.1 ML. This non-linear increase in activity towards the HER in alkaline media with increasing coverage is independent of the type of $TM(OH)_2$ and significantly differs from the linear enhancement found for Pt(111) with various, low amounts of $Ni(OH)_2$. Even more intriguingly, Pt(111) decorated with nano-islands of 3d $TM(OH)_2$, exhibit a clear activity trend following Ni > Co > Fe > Mn [10,11], whereas for modified Cu(111) a larger enhancement in reactivity for $Co(OH)_2$ over $Ni(OH)_2$ is observed. Therefore, a clear connection between the oxophilicity of the $TM(OH)_2$ and the activity cannot be made in the case of Cu(111).

Higher amounts of Cu(I) species, that may result from the Cu surface preparation, and hence a higher surface oxophilicity, have been reported to lead to a significant enhancement in the HER activity in alkaline electrolytes [23]. To evaluate the effect of $TM(OH)_2$ modification on the oxidation state of Cu(111), quasi in situ X-ray photoelectron spectroscopy (XPS) [24] was employed (Fig. 2). For this, the deposition and the cyclic voltammetry were performed inside an Ar-filled glove box, and the electrodes were emersed from the electrochemical cell under potential control (0 V_{RHE}) before being transported to the XPS chamber without any contact to air (see Supporting Information (SI)). Fig. 2a and b show the Cu LMM Auger signals for Cu(111) modified with $Ni(OH)_2$ and $Co(OH)_2$, respectively, which can be used to determine the relative population of different oxidation states, i.e., Cu(0) and Cu(I), via the relative intensities of the peaks [23,25]. The relative intensities of the highest peak appearing at a kinetic energy of ~ 919.0 eV associated with Cu(0) species [26], and the peak at ~ 916.5 eV attributed to Cu(I) species [26], remain unaltered for all the samples, i.e., Cu(0) >> Cu(I). Therefore, sub-monolayer modifications of Cu(111) with $Ni(OH)_2$ and $Co(OH)_2$, leave its oxidation state unchanged at Cu(0), and the observed activity enhancement cannot be attributed to higher amounts of Cu(I) species. The presence of oxidized Ni species on the surface is confirmed by the presence of the small signals in the Ni 2p region at binding energies (BE) of

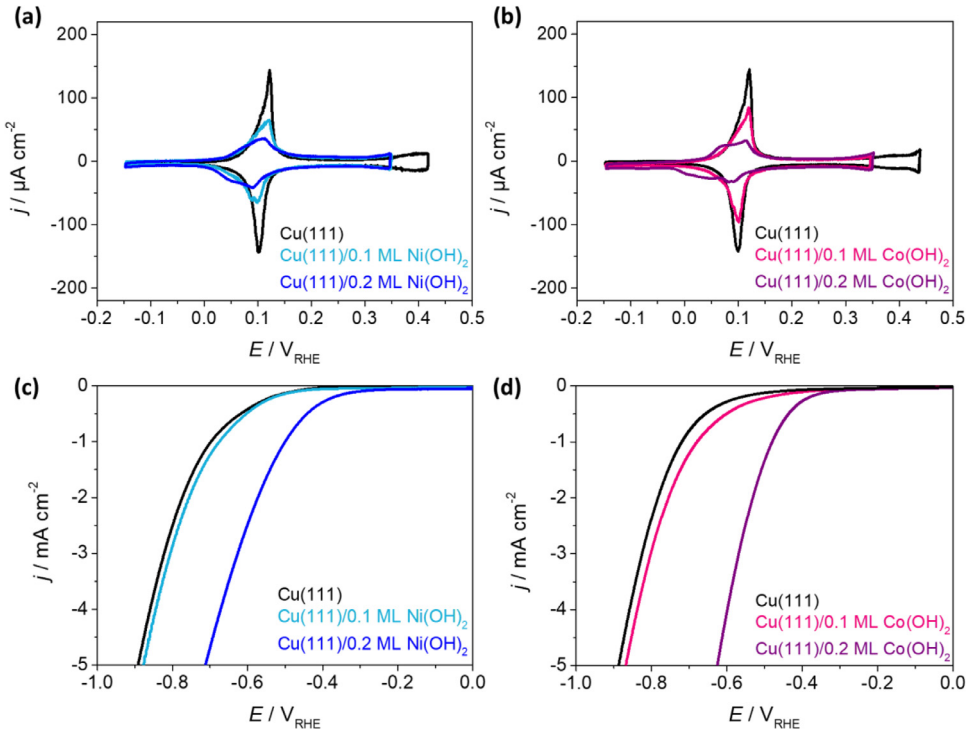

Fig. 1. Electrochemical behavior of $Ni(OH)_2$ and $Co(OH)_2$ modified Cu(111) electrodes. Fingerprint cyclic voltammograms (CVs) for (a) Cu(111) with 0.1 ML and 0.2 ML $Ni(OH)_2$ and (b) Cu(111) with 0.1 ML and 0.2 ML $Co(OH)_2$ in 0.1 M NaOH with a scan rate of 50 mV/s. Panel (c) and (d) show the HER activities in 0.1 M NaOH for Cu(111) modified with 0.1 ML and 0.2 ML $Ni(OH)_2$, and Cu(111) modified with 0.1 ML and 0.2 ML $Co(OH)_2$, respectively. Black lines: Cu(111) reference. (For interpretation of the references to colour in their figure legend, the reader is referred to the web version of this article.)

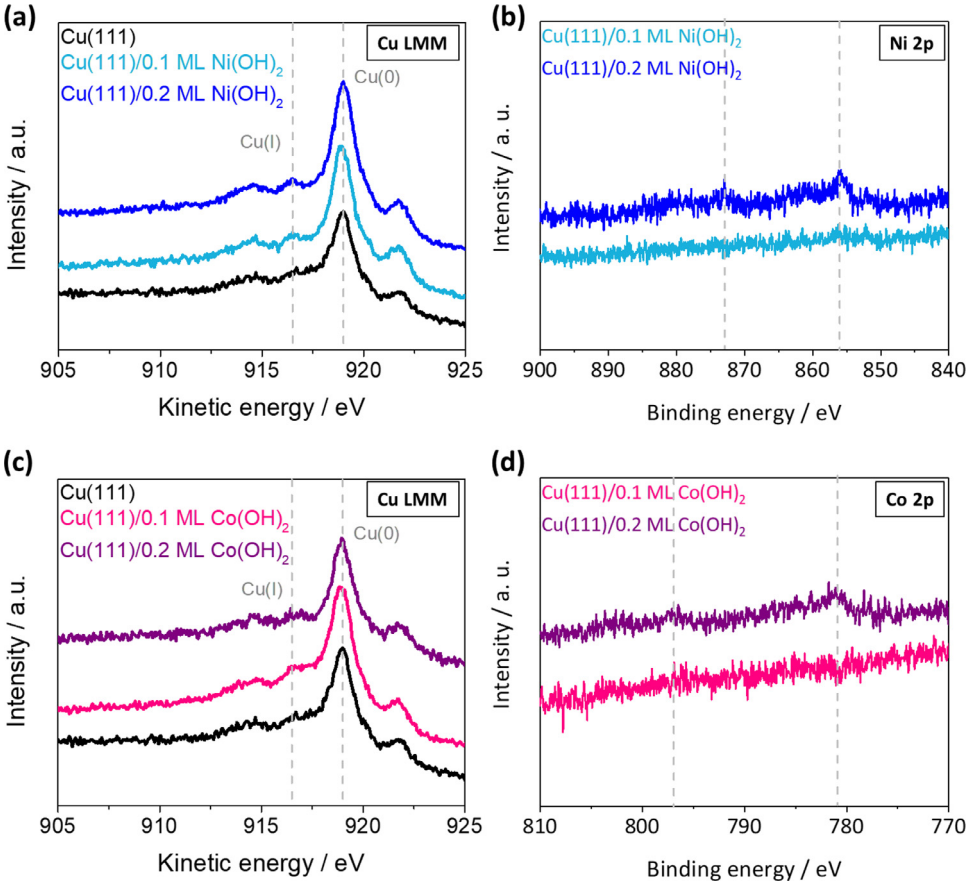

Fig. 2. Quasi in situ X-ray photoelectron spectroscopy: Cu LMM Auger signals for Cu(111) with different coverages of (a) $Ni(OH)_2$ and (c) $Co(OH)_2$. (b) XPS spectra of the Ni 2p region and (d) of the Co 2p region. All spectra were recorded with a take-off angle of 60° between the Cu(111) surface normal and the analyzer.

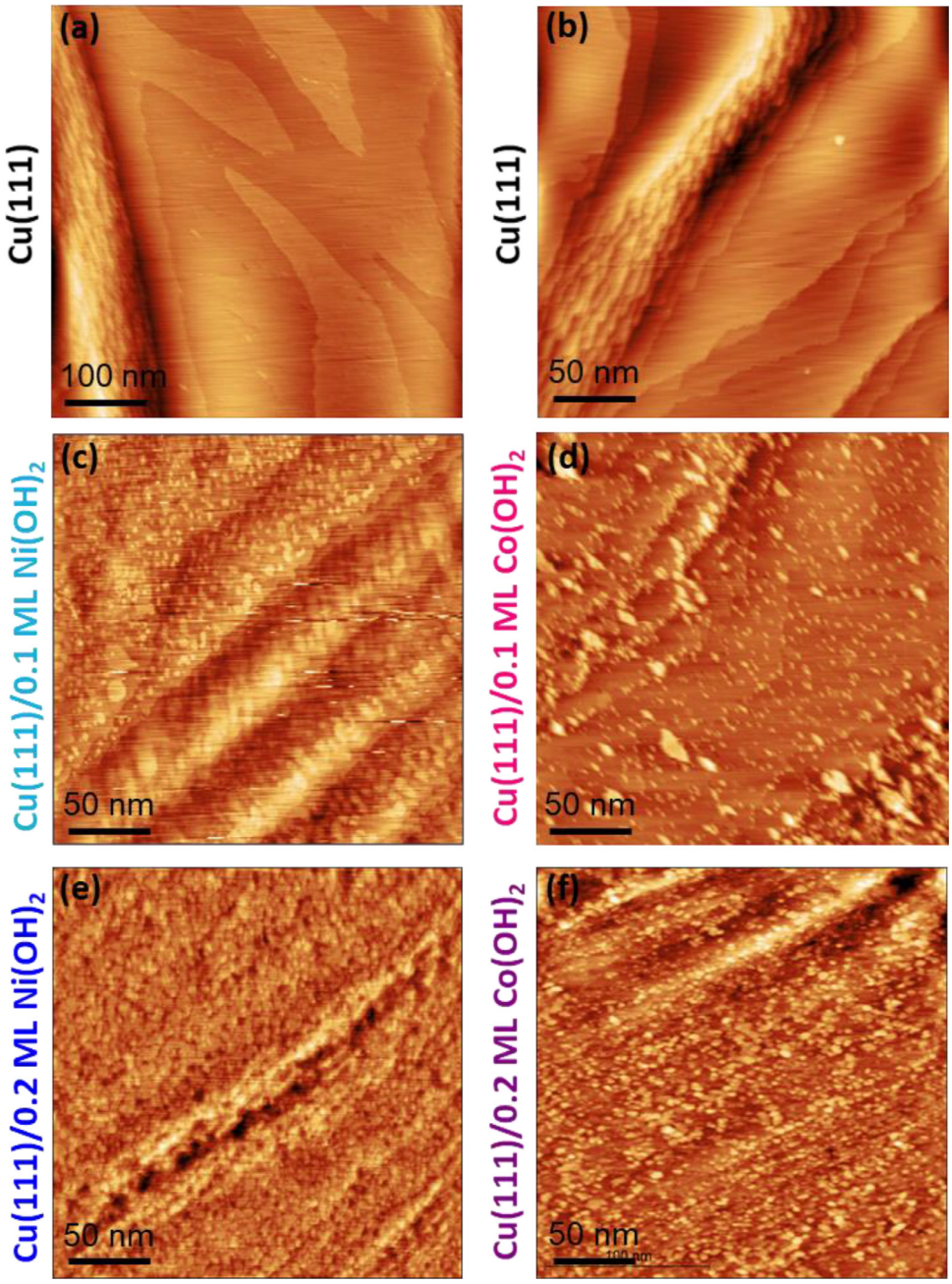

Fig. 3. In situ EC STM images of (a)-(b) metallic Cu(111), (c)-(d) Cu(111) with 0.1 ML $Ni(OH)_2$ and 0.1 ML $Co(OH)_2$ and (e)-(f) Cu(111) with 0.2 ML $Ni(OH)_2$ and 0.2 ML $Co(OH)_2$, respectively, at -0.05 V_{RHE} in 0.1 M NaOH. Image sizes are (500 × 500) nm^2 (a) and (250 × 250) nm^2 (b-f). I_{tip}=1 nA, E_{tip}= 0.25 V_{RHE}.

~ 856 eV and 873 eV (Fig. 2b), which correspond to Ni $2p_{3/2}$ and Ni $2p_{1/2}$, and which is in good agreement with literature values for $Ni(OH)_2$ [27,28]. Similar XPS results are obtained for $Co(OH)_2$ modified Cu(111), where the small peaks at ~781 eV (Co $2p_{3/2}$) and 796 eV (Co $2p_{5/2}$) clearly indicate the presence of $Co(OH)_2$ at the surface (Fig. 2d) [28]. Both the adsorbed Ni and Co species are therefore interpreted as hydroxides that do not get reduced or oxidized in the present systems. The same behavior is known for irreversibly adsorbed $Ni(OH)_2$ and $Co(OH)_2$ on Pt in its pseudocapacitive potential region [10,13].

Both the unusual non-linear activity trend with increasing coverages and the enhanced performance of $Co(OH)_2$ over $Ni(OH)_2$ modified Cu(111), are significant differences compared to Pt(111) based electrocatalysts. This cannot be attributed to the oxophilicity of the Cu surface, as was ruled out by the XPS results, nor to the oxophilicity of the $TM(OH)_2$ itself, as was previously discussed for Pt [10,23]. However, it is well known, that Cu is highly prone to surface restructuring processes, not only upon anion adsorption [29–32] or during electrocatalytic reactions (e.g. CO oxidation [33] and reduction [34–36] or hydrogen evolution in acidic media [37,38]), but even at its pzfc [21]. If we compare the much lower cohesive energy of Cu of 3.5 eV with that of Pt (5.84 eV) [39], it seems likely, that the modification of Cu(111) with $TM(OH)_2$ has a different effect on its structure and/or morphology. While ex situ scanning tunneling microscopy of the as-prepared Pt(111) modified with $Ni(OH)_2$ and $Co(OH)_2$ has revealed the presence of randomly distributed, three-dimensional clusters, consisting of approximately two $TM(OH)_2$ layers [8,10], our previous results evidence a disintegration of the Cu(111) surface upon $Ni(OH)_2$ deposition [22]. To get a realistic picture and to compare the structure and morphology

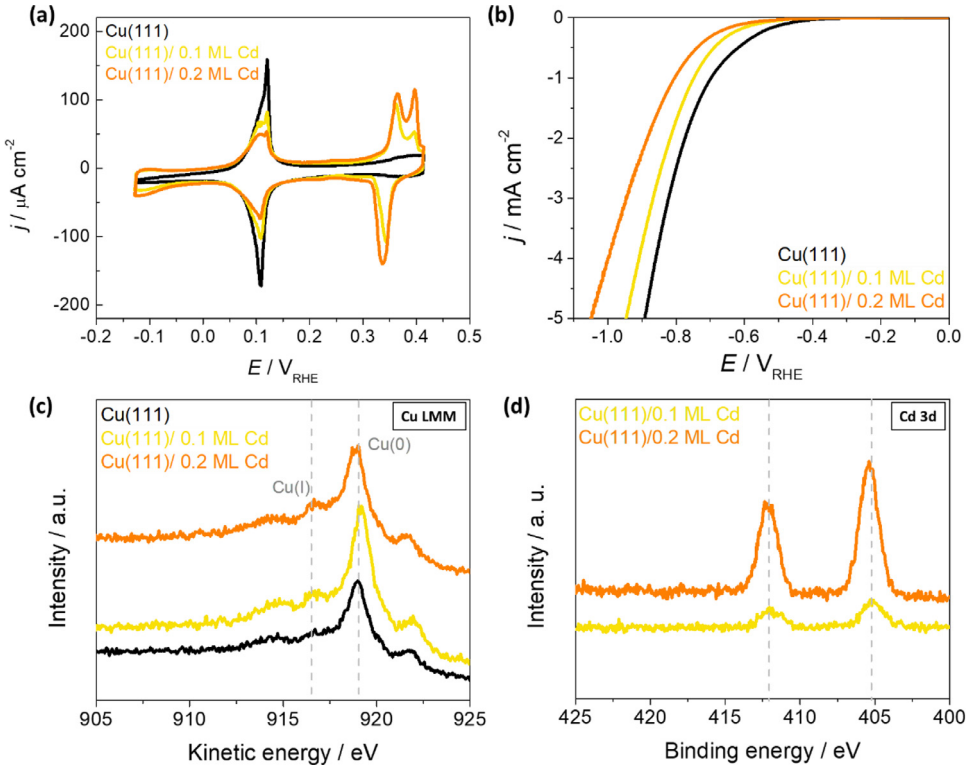

Fig. 4. (a) Fingerprint CVs and (b) the corresponding HER activities for Cu(111) with 0.1 ML and 0.2 ML of Cd. Black lines correspond to the measurement of blank Cu(111). (c) Cu LMM Auger signals and (d) XPS spectra of the Cd 3d region for Cu(111) with different coverages of Cd. (For interpretation of the references to colour in their figure legend, the reader is referred to the web version of this article.)

of the different, sub-monolayer modified Cu(111), we performed in situ EC-STM.

Fig. 3a and b depict the metallic Cu(111) surface in 0.1 M NaOH at -0.05 V_{RHE} in two different magnifications, which reveal a surface morphology consisting of flat terraces separated by either monolayer steps (~ 0.22 nm) or step bundles. Upon adding 0.1 ML of $Ni(OH)_2$, the Cu(111) morphology changes and adopts a rougher appearance, affected by numerous Cu islands with a specific height of around 0.20 nm (see Fig. 3c and Fig. S2), as was previously shown [22]. A higher coverage of 0.2 ML of $Ni(OH)_2$, leads to an even more pronounced restructuring of the surface with a further increased island density and a three-dimensional (3D) roughening (Fig. 3e). Cu is known to be very mobile, which is attributed to Cu ad-atoms (Cu_{ad}), detached from under-coordinated sites, that aggregate to small clusters [40]. This effect is enhanced in the presence of adsorbates that act as surfactants and that stabilize these clusters, such as CO, and has been observed at the solid/liquid [33] and the solid/gas interface [39,41,42]. It seems plausible that $Ni(OH)_2$ binds to low-coordinated Cu atoms in a similar fashion, forming mobile $Ni(OH)_2$-Cu_{ad} complexes, which likewise causes an increased mobility of the Cu(111) surface and leads to the observed disintegration [22]. We assume that $Ni(OH)_2$ is adsorbed at the Cu step edges and stabilizes the roughened surface by lowering the step edge formation energy, even though it is not directly locatable with the EC-STM.

Cu(111) modified with 0.1 ML $Co(OH)_2$ reveal a cluster like morphology, where evenly distributed 3-5 nm small islands reside on top of the terraces and some larger 3D islands are preferably located at step bundles (see Fig. 3d). This indicates different local coverages, which is in contrast to $Ni(OH)_2$. The clusters exhibit sphere-like, round morphologies with heights of approximately 0.65 – 1.20 nm (see Fig. S2). Due to the absence of the characteristic monoatomic height and thermodynamic shape of Cu ad-islands, we conclude that the $Co(OH)_2$ is visualized in the EC-STM, and that it predominantly forms 3D islands with 2 – 4 $Co(OH)_2$ layers height [10]. An increase of the coverage to 0.2 ML of $Co(OH)_2$, causes an increase in number and size of these islands, similar to what was found for Sn modified Au(111) electrodes [43]. However, while Sn islands coalesce on Au(111) and form merged 2D structures during longer immersion times, it is mostly the number of uniformly distributed $Co(OH)_2$ clusters that significantly increases with increasing Co^{2+} ion concentrations. These clusters exhibit the same approximate height of around 0.65 – 0.95 nm. It is not understood why modification with $Ni(OH)_2$ and with $Co(OH)_2$ leads to different types of restructuring. One possible reason for the formation of the 3D $Co(OH)_2$ cluster could result from its preference for a Volmer-Weber type growth, i.e., a higher tendency to cluster, caused by stronger bonds between the foreign species or by a higher rate of surface nucleation compared to diffusive processes [44]. It is important to note that on Pt(111) such a growth mechanism was observed for both $Ni(OH)_2$ and $Co(OH)_2$ [8,10]. The significant differences in the nature of the deposition and the morphological characteristics between Cu(111) modified with $Ni(OH)_2$ and $Co(OH)_2$ can help to rationalize the unexpected activity trend $Co(OH)_2$ > $Ni(OH)_2$ on Cu(111).

The decoration of Cu(111) with different $TM(OH)_2$ species provides the possibility to tune the catalyst's activity towards the HER in alkaline media due to an inherent change of the electrocatalytic properties. Chemically, this clearly induces oxophilic sites that are expected to influence the catalytic performance of these bimetallic systems. In addition, in order to study the changes induced by a metallic species, we irreversibly adsorbed sub-monolayers of Cd on Cu(111). Cd can be reversibly deposited via UPD on Cu(111) and Cu(100) in acidic chloride containing solutions [17,45], which makes it likely that an irreversible adsorption on Cu(111) is possible in alkaline solutions. Fig. 4a depicts the fingerprint CV of

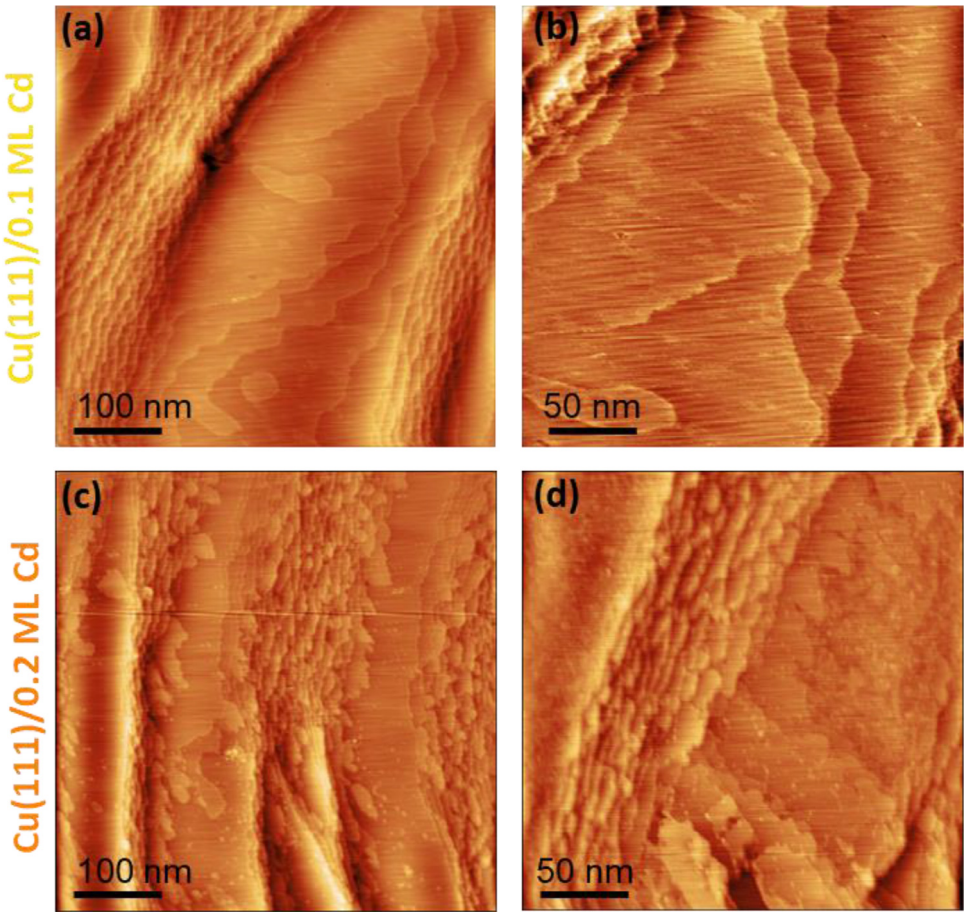

Fig. 5. In situ EC STM images of Cu(111)/0.1 ML Cd and Cu(111)/0.2 ML Cd at −0.05 V_{RHE} in 0.1 M NaOH. STM images of each Cd modified Cu(111) surface are represented in two different magnifications. Image sizes are (500 × 500) nm^2 (a,c) and (250 × 250) nm^2 (b,d). I_{tip}=1 nA, E_{tip}= 0.25 V_{RHE}.

Cu(111) with 0.1 ML and 0.2 ML Cd in 0.1 M NaOH. The estimation of the apparent coverage was carried out similarly as described for the $TM(OH)_2$ species (see Fig. S3 and Tables S2-3). Interestingly, in contrast to adsorbed $Ni(OH)_2$ and $Co(OH)_2$, the Cd undergoes a redox process as indicated by the anodic double peak and corresponding cathodic peak in the potential range between 0.30 and 0.45 V_{RHE}. Such redox reactions have been previously reported for various metals irreversibly adsorbed on Pt, such as Bi, Sb, As and Pb [4]. Previous works explain the redox reactions of these adatoms as a change in oxidation state from zero, i.e., totally discharged, to a higher value upon the positive-going potential sweep, where both the reduced and oxidized species are adsorbed on the Pt [4]. The charge of the reduction peak of oxidized Cd at 0.34 V_{RHE} reveals coverages that are slightly smaller but in reasonable agreement with those estimated from the OH adsorption charges (see Table S3).

The electrocatalytic properties of Cd modified Cu(111) towards the HER in alkaline solution are shown in Fig. 4b. While $Ni(OH)_2$ and $Co(OH)_2$ modifications clearly generate a promoting effect for the HER, we find a decrease in activity for both 0.1 and 0.2 ML Cd coverage.

The chemical composition of Cd modified Cu(111) is examined with quasi in situ XPS (see Fig. 4). Similar to what was found for the $TM(OH)_2$/Cu(111) electrodes, the Cu surface stays mostly metallic upon deposition of sub-monolayer amounts of Cd, which is determined by the relative intensities of Cu(0) >> Cu(I) in the Auger signals (see Fig. 4c). The Cd 3d region, shown in Fig. 3d, clearly reveals the presence of Cd species on the surface. Where the observed peaks with positions at around 405 and 412 eV, corresponding to Cd $3d_{5/2}$ and $3d_{3/2}$, with a spin orbit splitting of around 7 eV, are consistent with literature values reported for metallic Cd [46,47]. However, it has to be noted that metallic Cd cannot be unambiguously distinguished from any oxidized Cd species using XPS due to the high similarity in binding energies. The results therefore cannot unambiguously refute the possibility of having $Cd(OH)_2$ nor that of a Cu-Cd alloy formation.

In situ EC-STM imaging of 0.1 ML Cd on Cu(111) reveals that the Cd first deposits at step sites, which leads to a bright appearance of the step edges (Fig. 5a and b). Additional bright features on the terraces (Fig. 5b) can be attributed to adsorbed Cd. While the step edges look sharp, the features on top of the terraces appear fuzzy indicating a certain mobility. 0.2 ML of Cd trigger the formation of small, clearly separated clusters on the terraces and the decoration of the step edges. EC-STM data that show the surface morphology and structure evolution over time, after Cd deposition, indicate strong surface dynamics where extensive 2D clustering of the surface is observed after prolonged imaging (for longer than 2 hours) at -0.05 V_{RHE} (see Fig. S4).

Oxidation of the adsorbed Cd at 0.36 V_{RHE} (see Fig. 4a) leads to the formation of large vacancy islands. This effect is even more pronounced at a more positive potential of 0.43 V_{RHE}, located after the second anodic peak (see Fig. S5). This surface morphology change during Cd oxidation suggests a dissolution process, which can be attributed to a strong bond between the deposited Cd and the Cu surface that causes disruption of the topmost surface upon oxidation, similar to what was found for irreversibly adsorbed Sn on Au(111) [43] or Sb on Pt(111) [48]. This process is found to be fully reversible in the present case (see Fig. S5).

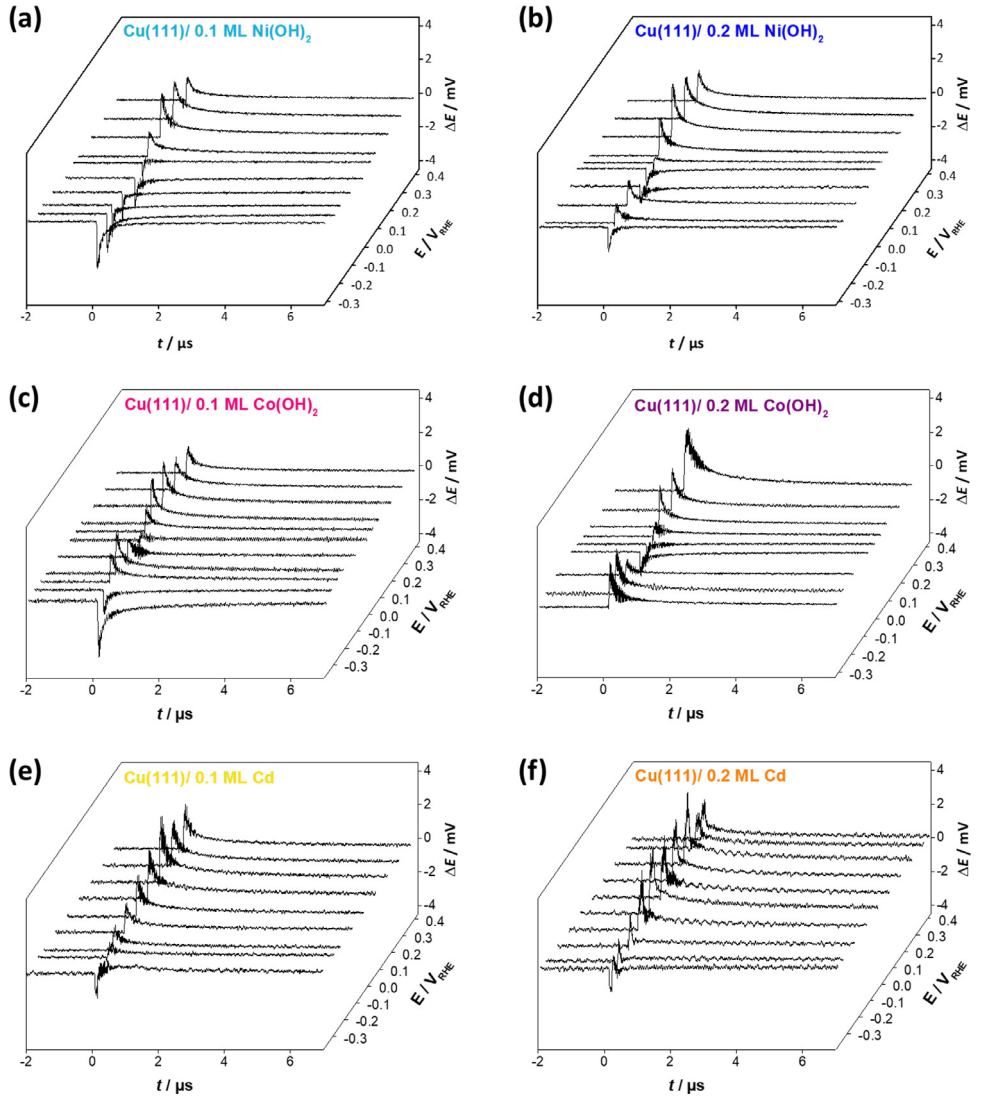

Fig. 6. 3D plots of the laser transients (ΔE vs t) recorded on Cu(111) with different adatom coverages within the approximate potential range of -0.4 to 0.4 V_{RHE}. (a)-(b) 0.1 ML and 0.2 ML $Ni(OH)_2$, (c)-(d) 0.1 ML and 0.2 ML $Co(OH)_2$, and (e)-(f) 0.1 ML and 0.2 ML Cd.

While we previously focused on the electrocatalytic properties as well as the structure and morphology of the modified Cu(111) electrodes, knowledge of the position and evolution of the pme upon adatom deposition is highly desirable. The pme is closley related to the pzfc and therefore a central parameter for the understanding of electrocatalytic activity, due to the insights it provides on the specific interactions of the interfacial water molecules with the electrode [5]. Therefore, the laser-induced temperature jump method was employed to shed light on the interfacial water reorganization and its impact on the HER activities of differently modified Cu(111) electrodes in alkaline media. The determination of the pme value and the thermal coefficients for bare Cu(111) single crystals in 0.1 M NaOH can be found in refs [19,22]. The laser-induced potential transients of all the investigated electrodes are shown in Fig. 6. In all cases, at sufficiently high potentials (approximately between 0.35 and 0.1 V_{RHE}) the transients are positive, indicating that the interfacial water adlayer has a net orientation with their negative end, i.e., the oxygen, towards the metal. At the onset of the OH adsorption peak at around 0.06-0.09 V_{RHE} the transients for Cu(111) with $Ni(OH)_2$ and $Co(OH)_2$ change their sign to negative, i.e., the hydrogen-towards-the-metal configuration is favored, as was previously found for bare Cu(111) [19,21]. Intriguingly, for both $TM(OH)_2$/Cu(111) electrodes at even more negative potentials, the transients become positive again in a quite narrow potential region, before changing to negative once more. While for $Co(OH)_2$, the appearance of three turn-overs of the water adlayer are found, independently of the coverage, $Ni(OH)_2$ shows this behavior for the higher coverage, i.e., 0.2 ML, only. The transients of Cd modified Cu(111) reveal that there is only one change in the orientation of the interfacial water molecules, which is shifted to lower potentials of approximately -0.15 V_{RHE} (Fig. 6e and f).

The laser-induced potential transients provide insight into the electric field at the solid/liquid interface, which is accessible through determination of the thermal coefficient of the potential drop across the double layer ($\partial\Delta\phi/\partial T$). This parameter can be extracted from the slope of a suitable linearized plot of the transients (see description in the Supporting Information and Fig. S6) and are depicted in Fig. 7a. The potential of zero response (pzr), where $(\frac{\partial\Delta\phi}{\partial T})_q = 0$, corresponds to a maximum disorder in the interfacial water layer and the turn-over of the water molecules, which is generally attributed to the pme of double layer formation [5]. The pme is closely linked to the pzfc, where the electric field across the interface is zero, which generates a random orientation of the water dipoles [14,15]. Detailed information is provided in the SI.

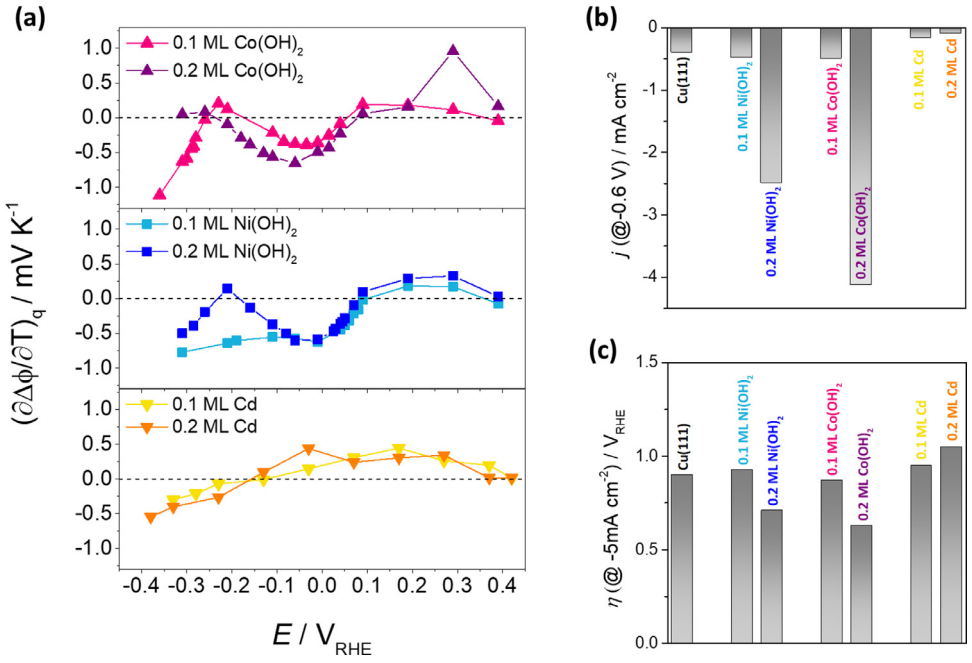

Fig. 7. (a) Thermal coefficient ($\partial\Delta\phi/\partial T$) for Cu(111) modified with $Ni(OH)_2$, $Co(OH)_2$ and Cd. Comparison of the HER activities expressed as (c) the current density at -0.6 V_{RHE} and (d) the overpotential at a current density of -5 mA cm^{-2}, extracted from potentiodynamic measurements at 50 mVs^{-1}.

The measured thermal coefficients have to be adjusted by the contribution of the thermodiffusion potential ($\sim$ -0.43 mV K^{-1}) [49], which must be accounted for due to the high OH^- ion mobility (Fig. S7). If we compare the potential dependence of the thermal coefficient of $Ni(OH)_2$ and $Co(OH)_2$ modified Cu(111), we find a peak shaped development in the lower potential region close to the onset of the HER for coverages of 0.2 ML for both $TM(OH)_2$ and for 0.1 ML $Co(OH)_2$, whereas for 0.1 ML $Ni(OH)_2$ no second transition from negative to positive is observed. Consequently, for $Co(OH)_2$ on Cu(111), two pme values of double layer formation exist, independently of the coverage, while this is only the case for the higher coverage of $Ni(OH)_2$ on Cu(111) (see Fig. S8). The water orientation at the surface at a given potential is responsible for the appearance of pme values. The orientation is influenced by a heterogeneous chemical composition, or by a step versus terrace site adsorption and corresponding charge-dipole interactions through locally induced positive free charges at the steps causing an oxygen-towards-the-metal configuration [50]. In case of $Ni(OH)_2$ on Cu(111), the coverage critically dictates the trend of the thermal coefficient over the potential range of interest. Only higher coverages of 0.2 ML $Ni(OH)_2$ cause a degree of Cu(111) surface roughening that is high enough to induce a reorientation of the water dipoles [22]. The surface chemistry, locally changed through the presence of oxophilic $Ni(OH)_2$ that is assumed to preferentially reside at the step edges, certainly also contributes to the observed effect.

In case of $Co(OH)_2$, in situ EC-STM imaging upon irreversible adsorption suggests the formation of $Co(OH)_2$ islands rather than substrate restructuring that causes Cu ad-island growth. This type of nucleation leads to the development of a significantly higher local concentration of oxophilic sites, which can chemically favor an oxygen-towards-the-metal configuration at lower potentials and explains the appearance of a second pme independently of the coverage.

Intriguingly, when we compare the HER activities, considered as either the current density or the overpotential (η) (see Fig. 7b and c), we can clearly correlate the greater enhancement for $Co(OH)_2$ over $Ni(OH)_2$ with a decrease in the thermal coefficient, which is directly associated with the interfacial electric field strength [12]. For 0.1 ML $Co(OH)_2$ and $Ni(OH)_2$ not only the current density at -0.6 V_{RHE} (-0.48 and -0.5 mA cm^{-2}) and the overpotential at -5 mA cm^{-2} (0.93 and 0.87 V) are quite comparable, also the thermal coefficients shown in Fig. 7a close to the onset of the HER (i.e. -0.3 V_{RHE}) are almost identical. For surface concentrations of 0.2 ML $Ni(OH)_2$ and $Co(OH)_2$, however, the HER current densities at a scan rate of 50 mV/s (-2.2 versus -4.1 mA cm^{-2}) are enhanced by a factor of 6.3 and 10.3 relative to the bare Cu(111), respectively. The respective values of the thermal coefficients reflect this behavior well. At the onset of the HER, they are significantly negative for $Ni(OH)_2$, while they are close to zero for $Co(OH)_2$. This means that the highly disordered water ad-layer is only persistent at even lower potentials for 0.2 ML $Co(OH)_2$ on Cu(111), which explains the unexpected trend (Co > Ni) for Cu(111) modified electrodes.

For Cd modified Cu(111), we observe the presence of only one pme at approximately -0.15 V_{RHE}, which is shifted to lower potentials compared to pure Cu(111). There is only a small difference of 20 mV between the pme values for 0.1 and 0.2 ML coverages (see Fig. S8). For Cd modified Cu(111) the HER onset is shifted towards more negative values, therefore, this small shift of the pme towards more negative values, does not seem to have any influence on its reactivity, since we observe a significantly negative thermal coefficient at potentials close to the onset of the HER.

4. Conclusion

In conclusion, we have shown that it is possible to decorate Cu(111) using irreversible adsorption not only with sub-monolayers of different $TM(OH)_2$, but also with metallic Cd, which in contrast to $Ni(OH)_2$ and $Co(OH)_2$ exhibits a quasi-reversible redox reaction.

The behavior of all three bimetallic systems is predominantly influenced by the properties of Cu(111). This substrate has a tendency to restructure, and its reorganization is different with $Ni(OH)_2$, $Co(OH)_2$ and Cd. Therefore, the morphological/structural effects of the modification have to be thoroughly examined in the case of Cu(111) electrodes, before an understanding of the observed activity trends is possible. We find that the structural and the re-

lated chemical changes of the electrode surfaces are intimately related to the electric field at the solid/liquid interface and to the activity towards the HER.

In situ EC-STM data for Cu(111) modified with $Ni(OH)_2$ and $Co(OH)_2$ clearly reveal significant differences in the nature of the deposition and the morphological characteristics of the modified surfaces. While the addition of $Ni(OH)_2$ causes a drastic surface restructuring including Cu ad-island growth and a three-dimensional roughening at higher coverage, irreversible adsorption of $Co(OH)_2$ leads to nucleation and growth of three-dimensional $Co(OH)_2$ islands. This understanding of morphology and structure changes upon irreversible adsorption can help to rationalize the observed unusual activity trend $Co(OH)_2$ > $Ni(OH)_2$. There is a clear correlation of the thermal coefficient, i.e., the electric field strength, and the HER activities in alkaline media for these modified Cu(111) electrodes. The occurrence of a second pme at negative potentials close to the HER onset, as observed for 0.2 ML of $Ni(OH)_2$ and 0.1 and 0.2 ML of $Co(OH)_2$ generally indicates a higher activity towards this reaction. The significant decrease in the electric field strength, persisting towards cathodic potentials and over a wide potential range in case of high $Co(OH)_2$ coverages, correlates with the highest activity, which can be assigned to the greatest increase in disorder of the interfacial water ad-layer, which promotes the charge transfer through the double-layer.

The adsorption of Cd on Cu(111) initiates at step sites at early stages of the process, and surface alloying is assumed. The thermal coefficient in the HER potential range is shifted to more negative values compared to Cu(111), which is reflected in the rather negative shift of the HER onset.

In the three systems investigated in the present study, we found a clear correlation of the electric field at the solid/liquid interface and the activity towards the HER. The thermal coefficient accessible through laser-induced potential transient studies is therefore a meaningful descriptor for this reaction. It is generally essential for electrocatalysis research and development that this descriptor is found to be leastwise affected by the morphology, structure and chemistry of the respective electrode surface.

Declaration of Competing Interest

The authors declare that they have no known competing financial interests or personal relationships that could have appeared to influence the work reported in this paper.

Acknowledgment

A.A. is a recipient of a doctorate (DOC) Fellowship of the Austrian Academy of Sciences at the Institute of Physical Chemistry. C.G. thanks the Austrian Research Promotion Agency (FFG) for funding by the project number 870523. J.K-L. acknowledges funding by the Austrian Science Fund (FWF) via grant I-4114-N37. J.M.F and V.C. acknowledge financial support from Ministerio de Ciencia e Innovación (project PID2019-105653GB-100) and Generalitat Valenciana (project PROMETEO/2020/063).

Supplementary materials

Supplementary data associated with this article can be found, in the online version, at doi:10.1016/j.electacta.2021.139222.

References

[1] F. Calle-Vallejo, M.T.M.M. Koper, A.S. Bandarenka, Tailoring the catalytic activity of electrodes with monolayer amounts of foreign metals, Chem. Soc. Rev. 42 (2013) 5210–5230, doi:10.1039/c3cs60026b.
[2] R.C. Propst, Undervoltage effects in the determination of silver by scanning coulometry, J. Electroanal. Chem. 16 (1968) 319–326, doi:10.1016/0368-1874(68)87052-2.
[3] E. Herrero, L.J. Buller, H.D. Abruña, Underpotential deposition at single crystal surfaces of Au, Pt, Ag and other materials, Chem. Rev. 101 (2001) 1897–1930, doi:10.1021/cr9600363.
[4] J.M. Feliu, J.M. Orts, Irreversible adsorption of metal atoms in electrocatalysis, in: Fundam. Asp. Heterog. Catal. Stud. by Part. Beams, Plenum Press, 1991, pp. 57–62, doi:10.1007/978-1-4684-5964-7_5.
[5] N. García-Aráez, V. Climent, J.M. Feliu, Evidence of water reorientation on model electrocatalytic surfaces from nanosecond-laser-pulsed experiments, J. Am. Chem. Soc. 130 (2008) 3824–3833, doi:10.1021/ja0761481.
[6] P. Sebastián-Pascual, I. Jordão Pereira, M. Escudero-Escribano, Tailored electrocatalysts by controlled electrochemical deposition and surface nanostructuring, Chem. Commun. 56 (2020) 13261–13272, doi:10.1039/d0cc06099b.
[7] J.M. Feliu, E. Herrero, Formic acid oxidation, Handb. Fuel Cells. (2010), doi:10.1002/9780470974001.f206048.
[8] a R. Subbaraman, D. Tripkovic, D. Strmcnik, K.C. Chang, M. Uchimura, P. Paulikas, V. Stamenkovic, N.M. Markovic, Enhancing hydrogen evolution activity in water splitting by tailoring Li+-Ni(OH)2-Pt interfaces, Science 334 (2011) 1256–1260.
[9] N. Danilovic, R. Subbaraman, D. Strmcnik, K.-C. Chang, A.P. Paulikas, V.R. Stamenkovic, N.M. Markovic, Enhancing the alkaline hydrogen evolution reaction activity through the bifunctionality of $Ni(OH)_2$ /metal catalysts, Angew. Chemie. 124 (2012) 12663–12666, doi:10.1002/ange.201204842.
[10] R. Subbaraman, D. Tripkovic, K.C. Chang, D. Strmcnik, A.P. Paulikas, P. Hirunsit, M. Chan, J. Greeley, V. Stamenkovic, N.M. Markovic, Trends in activity for the water electrolyser reactions on 3d M(Ni,Co,Fe,Mn) hydr(oxy)oxide catalysts, Nat. Mater 11 (2012) 550–557, doi:10.1038/nmat3313.
[11] D. Strmcnik, P.P. Lopes, B. Genorio, V.R. Stamenkovic, N.M. Markovic, Design principles for hydrogen evolution reaction catalyst materials, Nano Energy 29 (2016) 29–36, doi:10.1016/j.nanoen.2016.04.017.
[12] I. Ledezma-yanez, W.D.Z. Wallace, P. Sebastián-Pascual, V. Climent, J.M. Feliu, M.T.M.M. Koper, Interfacial water reorganization as a pH-dependent descriptor of the hydrogen evolution rate on platinum electrodes, Nat. Energy. 2 (2017) 1–7, doi:10.1038/nenergy.2017.31.
[13] F.J. Sarabia, P. Sebastián-Pascual, M.T.M. Koper, V. Climent, J.M. Feliu, Effect of the interfacial water structure on the hydrogen evolution reaction on Pt(111) modified with different nickel hydroxide coverages in alkaline media, ACS Appl. Mater. Interfaces 11 (2019) 613–623, doi:10.1021/acsami.8b15003.
[14] V. Climent, B.A. Coles, R.G. Compton, Laser-induced potential transients on a Au(111) single-crystal electrode. determination of the potential of maximum entropy of double-layer formation, J. Phys. Chem. B. 106 (2002) 5258–5265, doi:10.1021/jp020054q.
[15] V. Climent, B.A. Coles, R.G. Compton, Coulostatic potential transients induced by laser heating of a Pt(111) single-crystal electrode in aqueous acid solutions. rate of hydrogen adsorption and potential of maximum entropy, J. Phys. Chem. B. 106 (2002) 5988–5996, doi:10.1021/jp020785q.
[16] Y.S. Chu, I.K. Robinson, A.A. Gewirth, Properties of an electrochemically deposited Pb monolayer on Cu(111), Phys. Rev. B - Condens. Matter Mater. Phys. 55 (1997) 7945–7954, doi:10.1103/PhysRevB.55.7945.
[17] S. Hümann, J. Hommrich, K. Wandelt, Underpotential deposition of cadmium on Cu(1 1 1) and Cu(1 0 0), Thin Solid Films 428 (2003) 76–82, doi:10.1016/S0040-6090(02)01276-2.
[18] A. Auer, J. Kunze-Liebhäuser, A universal quasi-reference electrode for in situ EC-STM, Electrochem. Commun. 98 (2019) 15–18, doi:10.1016/j.elecom.2018.11.015.
[19] P. Sebastián-Pascual, F.J. Sarabia, V. Climent, J.M. Feliu, M. Escudero-Escribano, Elucidating the structure of the Cu-alkaline electrochemical interface with the laser-induced temperature jump method, J. Phys. Chem. C. 124 (2020) 23253–23259, doi:10.1021/acs.jpcc.0c07821.
[20] A. Tiwari, H.H. Heenen, A.S. Bjørnlund, T. Maagaard, E. Cho, I. Chorkendorff, H.H. Kristoffersen, K. Chan, S. Horch, Fingerprint voltammograms of copper single crystals under alkaline conditions: a fundamental mechanistic analysis, J. Phys. Chem. Lett. 11 (2020) 1450–1455, doi:10.1021/acs.jpclett.9b03728.
[21] A. Auer, X. Ding, A.S. Bandarenka, J. Kunze-Liebhäuser, The potential of zero charge and the electrochemical interface structure of Cu(111) in alkaline solutions, J. Phys. Chem. C. 125 (2021) 5020–5028, doi:10.1021/acs.jpcc.0c09289.
[22] A. Auer, F.J. Sarabia, D. Winkler, C. Griesser, V. Climent, J.M. Feliu, J. Kunze-Liebhäuser, Interfacial water structure as a descriptor for its electro-reduction on $Ni(OH)_2$ modified Cu(111), ACS Catal 11 (2021) 10324–10332, doi:10.1021/acscatal.1c02673.
[23] P. Farinazzo Bergamo Dias Martins, P. Papa Lopes, E.A. Ticianelli, V.R. Stamenkovic, N.M. Markovic, D. Strmcnik, Hydrogen evolution reaction on copper: promoting water dissociation by tuning the surface oxophilicity, Electrochem. Commun. 100 (2019) 30–33, doi:10.1016/j.elecom.2019.01.006.
[24] A. Foelske-Schmitz, X-ray photoelectron spectroscopy in electrochemistry research, in: K. Wandelt (Ed.), Encycl. Interfacial Chem., Elsevier, 2018, pp. 591–606.
[25] G. Panzner, B. Egert, H.P. Schmidt, The stability of CuO and Cu2O surfaces during argon sputtering studied by XPS and AES, Surf. Sci. 151 (1985) 400–408.
[26] M.C. Biesinger, Advanced analysis of copper X-ray photoelectron spectra, Surf. Interface Anal. 49 (2017) 1325–1334, doi:10.1002/sia.6239.
[27] M.C. Biesinger, L.W.M. Lau, A.R. Gerson, R.S.C. Smart, The role of the Auger parameter in XPS studies of nickel metal, halides and oxides, Phys. Chem. Chem. Phys. 14 (2012) 2434–2442, doi:10.1039/c2cp22419d.
[28] M.C. Biesinger, B.P. Payne, A.P. Grosvenor, L.W.M. Lau, A.R. Gerson, R.S.C. Smart, Resolving surface chemical states in XPS analysis of first row transition metals,

oxides and hydroxides: Cr, Mn, Fe, Co and Ni, Appl. Surf. Sci. 257 (2011) 2717–2730, doi:10.1016/j.apsusc.2010.10.051.
[29] V. Maurice, H.-H. Strehblow, P. Marcus, Situ STM study of the initial stages of anodic oxidation of Cu(111) in aqueous solution, Surf. Sci. 458 (2000) 185–194, doi:10.1149/1.1576225.
[30] J. Kunze, V. Maurice, L.H. Klein, H.H. Strehblow, P. Marcus, situ STM study of the effect of chlorides on the initial stages of anodic oxidation of Cu(111) in alkaline solutions, Electrochim. Acta. 48 (2003) 1157–1167, doi:10.1016/S0013-4686(02)00826-5.
[31] P. Broeckmann, M. Wilms, M. Arenz, A. Sp, K. Wandelt, Atomic structure of Cu (111) surfaces, in Dilute Sulfuric Acid Solution 199 (2003) 141–199.
[32] M. Arenz, P. Broekmann, M. Lennartz, E. Vogler, K. Wandelt, In-situ characterization of metal/electrolyte interfaces: sulfate adsorption on Cu(111), Phys. Status Solidi Appl. Res. 187 (2001) 63–74, doi:10.1002/1521-396X(200109)187:1<63::AID-PSSA63>3.0.CO;2-3.
[33] A. Auer, M. Andersen, E.M. Wernig, N.G. Hörmann, N. Buller, K. Reuter, J. Kunze-Liebhäuser, Self-activation of copper electrodes during CO electrooxidation in alkaline electrolyte, Nat. Catal. 3 (2020) 797–803, doi:10.1038/s41929-020-00505-w.
[34] G.H. Simon, C.S. Kley, B.R. Cuenya, Potential-dependent morphology of copper catalysts during CO2, Electroreduct. Reveal. In Situ Atomic Force Microscopy Res. Articles (2021) 2561–2568, doi:10.1002/anie.202010449.
[35] Y.G. Kim, A. Javier, J.H. Baricuatro, D. Torelli, K.D. Cummins, C.F. Tsang, J.C. Hemminger, M.P. Soriaga, Surface reconstruction of pure-Cu single-crystal electrodes under CO-reduction potentials in alkaline solutions: a study by seriatim ECSTM-DEMS, J. Electroanal. Chem. 780 (2016) 290–295, doi:10.1016/j.jelechem.2016.09.029.
[36] J. Huang, N. Hörmann, E. Oveisi, A. Loiudice, G.L. De Gregorio, O. Andreussi, N. Marzari, R. Buonsanti, Potential-induced nanoclustering of metallic catalysts during electrochemical CO_2 reduction, Nat. Commun. 9 (2018) 1–9, doi:10.1038/s41467-018-05544-3.
[37] H. Matsushima, A. Taranovskyy, C. Haak, Y. Gründer, O.M. Magnussen, Y. Gründer, O.M. Magnussen, Y. Gründer, O.M. Magnussen, Reconstruction of Cu(100) electrode surfaces during hydrogen evolution, J. Am. Chem. Soc. 131 (2009) 10362–10363, doi:10.1021/ja904033t.
[38] T.M.T. Huynh, P. Broekmann, From insitu towards inoperando conditions: scanning tunneling microscopy study of hydrogen intercalation in Cu(111) during hydrogen evolution, ChemElectroChem 1 (2014) 1271–1274, doi:10.1002/celc.201402147.
[39] B. Eren, D. Zherebetskyy, L.L. Patera, C.H. Wu, H. Bluhm, C. Africh, L.-W.W. Wang, G.A. Somorjai, M. Salmeron, Activation of Cu(111) surface by decomposition into nanoclusters driven by CO adsorption, Science 351 (2016) 475–478, doi:10.1126/science.aad8868.
[40] M. Poensgen, J.F. Wolf, J. Frohn, M. Giesen, H. Ibach, Step dynamics on Ag(111) and Cu(100) surfaces, Surf. Sci. 274 (1992) 430–440, doi:10.1016/0039-6028(92)90848-Z.
[41] B. Eren, D. Zherebetskyy, Y. Hao, L.L. Patera, L.W. Wang, G.A. Somorjai, M. Salmeron, One-dimensional nanoclustering of the Cu(100) surface under CO gas in the mbar pressure range, Surf. Sci. 651 (2016) 210–214, doi:10.1016/j.susc.2016.04.016.
[42] M. Roiaz, L. Falivene, C. Rameshan, L. Cavallo, S.M. Kozlov, G. Rupprechter, Roughening of Copper (100) at elevated CO pressure: Cu adatom and cluster formation enable CO dissociation, J. Phys. Chem. C. 123 (2019) 8112–8121, doi:10.1021/acs.jpcc.8b07668.
[43] L.A. Meier, D.R. Salinas, J.M. Feliu, S.G. García, Spontaneous deposition of Sn on Au(111). An in situ STM study, Electrochem. Commun. 10 (2008) 1583–1586, doi:10.1016/j.elecom.2008.08.013.
[44] L.G. Benning, G.A. Waychunas, Nucleation, growth, and aggregation of mineral phases: mechanisms and kinetic controls, in: S.L. Brantley, J.D. Kubicki, A.F. White (Eds.), Kinet. Water-Rock Interact, Springer Science+Business, 2008, pp. 259–334, doi:10.1007/978-0-387-73563-4_9.
[45] J. Hommrich, S. Hümann, K. Wandelt, Cadmium underpotential deposition on Cu(111): In situ scanning tunneling microscopy, Faraday Discuss. 121 (2002) 129–138, doi:10.1039/b200406m.
[46] J.F. Moulder, W.F. Stickle, P.E. Sobol, K.D. Bomben, Handbook of X-ray Photoelectron Spectroscopy, Perkin-Elmer Corp, Eden Prairie, MN, 1992.
[47] C.D. Wagner, A.V. Naumkin, A. Kraut-Vass, J.W. Allison, C.J. Powell, J.R.J. Rumble, NIST standard reference database, Version 3.4 (web version) 20 (2003), http://srdata.nist.gov/xps/.
[48] V. Climent, E. Herrero, J.M. Feliu, Electrocatalysis of formic acid and CO oxidation on antimony-modified Pt(111) electrodes, Electrochim. Acta. 44 (1998) 1403–1414, doi:10.1016/S0013-4686(98)00263-1.
[49] C.G. Vayenas, Interfacial Phenomena in Electrocatalysis, in: R.E. White, C.G. Vayenas, M.E. Gamboa-Aldeco (Eds.), Mod. Asp. Electrochem., Springer, New York, 2011.
[50] N. García-Aráez, V. Climent, J.M. Feliu, Potential-dependent water orientation on Pt(111) stepped surfaces from laser-pulsed experiments, Electrochim. Acta. 54 (2009) 966–977, doi:10.1016/j.electacta.2008.08.016.